Advances in Machinery, Materials Science and Engineering Application
M. Chen et al. (Eds.)

doi:10.3233/ATDE220434

Effect of B_4C on the Microstructure and Mechanical Properties of SiC Refractory Ceramics

Jiaxin CHEN [a], Pingan CHEN [a], Xiangchen LI [a,1], Yingli ZHU [a] and Feng WANG [b]
[a] *The State Key Laboratory of Refractories and Metallurgy, Wuhan University of Science and Technology, Wuhan 430081, China*
[b] *Qingdao Almatis Co., Ltd., Qingdao 266510, China*

Abstract. In this paper, the effect of B_4C content and heat treatment temperature on microstructure, mechanical properties and oxide resistance of SiC refractory ceramics were investigated. The results show that the inclusion of B_4C could improve the crystallinity of gengerated SiC and graphitization. When the B_4C content was 6%, the linear change of SiC-based refractory ceramics after heat treatment at 1450 °C decreased from 1.39% to 0.58%. At the same time, the cold modulus of rupture and cold compressive strength increased by 1.8 times and 2 times, respectively. Meanwhile, with the increase of B_4C content, the oxidation index of the SiC-based refractory ceramics decreased from 30.33% to 16.63% after oxidation at 1400 °C.

Keywords. SiC-based refractory ceramics, boron carbide (B_4C), mechanical properties, oxidation resistance

1. Introduction

Silicon carbide has good wear resistance and self-protection between 1300-1500°C; so it is intensively utilized as a special refractory material in severely scoured and corroded areas, such as blast furnaces and ironmaking furnaces. [1-3]. Although SiC based refractory ceramics have the above excellent properties, when the oxidation temperature reaches above 1200 °C, the oxidation product of SiC will undergo crystalline transformation, accompanied by volume expansion resulting in cracks which exhibits inferior oxidation resistance.

To solve the oxidation of SiC-based refractory materials, carbides, borides, and metal alloys are usually added as antioxidants [4-6]. B_4C is one of the most extensive non-oxide materials with low relative density (2.51 g/cm^3), extremely high hardness (only after diamond and cubic boron nitride), good wear resistance, and excellent thermal stability [7-8]. Meanwhile, B_4C will be oxidized to liquid phase B_2O_3 above 600 °C, which can restort cracks to improve the mechanical properties [9-10]. Magnani et al [11] incorporated 5% of B_4C as a sintering aid in the pressureless sintering of α-SiC, which could improve the sintering rate of SiC and inhibit the growth of SiC grains, thus enhancing the mechanical properties at 1500 °C. Ma et al [12] investigated the effect of

[1] Xiangchen Li, Corresponding author, The State Key Laboratory of Refractories and Metallurgy, Wuhan University of Science and Technology, Wuhan 430081, China; E-mail: lixiangcheng@wust.edu.cn.

B_4C content on the densification of ZrB_2 and found that B_4C could remove oxidized impurities during solid-phase sintering; moreover, when B_4C was included at 5%, the composite still had good oxidation resistance at 1500 °C. Fan et al [13] introduced B_4C into C/C-SiC three-dimensional materials. The uniform distribution of B_4C can both enhance the interfacial bonding with fibres and play an important role in the reinforcement of ceramic particles. At the same time, B_4C is more susceptible to oxidation to B_2O_3 at high temperatures, which can fill pores, cracks and other defects and improve the oxidation resistance of C/C-SiC.

Herin, The effects of B_4C content at 1100 ºC and 1450 ºC on the microstructure, mechanical properties and oxidation resistance of SiC-based refractory ceramics were investigated. The results show that B_4C can improve the crystallinity of generated SiC as well as graphitization, which can contribute to the improvement of mechanical properties and oxidation resistance.

2. Experiment

The raw materials were 63-72 wt.% SiC powders (~80 μm), 9 wt% Al-Si alloy powders (~48 μm), 8 wt% calcined Al_2O_3 micronized powders (~5 μm), 5 wt% flake graphite, 0-9 wt% B_4C powders (~20 μm), 6 wt% thermosetting phenolic resin as binding agent, and nickel nitrate hexahydrate as admixture. After each raw material was mixed well, the powder was pressed into cylindrical samples of Φ36 mm and strip samples of 140×25×25 mm at a pressure of 180 MPa. The pressed samples were cured at 200 ºC for 24 h, and then the cured samples were heat treated at 1100 ºC and 1400 ºC for 3 h under the atmosphere of buried carbon (coke), respectively.

The X'pert pro X-ray diffractometer, Nova NanoSEM 400 scanning electron microscope and INCA IE350 PentaFET X-3 energy spectrometer and Renishaw in Via Qontor Raman spectrometer were used to analyze the phase composition and microstructure. The bulk density, apparent porosity were measured by Archimedes principle. The cold modulus of rupture was tested using the 3-point bending method with a span of 125 mm and a loading rate of 0.15 MPa/min. The cold compressive strength was examined using YES-2000 digital display pressure tester.

3. Results and Discussions

3.1. Phase Composition and Microstructure of SiC-based Refractory Ceramics

Figure 1 shows the XRD patterns of the SiC-based refractory ceramics after heat treatment at 1100 °C and 1450 °C for different B_4C contents, respectively. From figure 1, it can be seen that the main crystalline phase of SiC-based refractory ceramics is SiC phase, which contains small amounts of graphite and Al_2O_3. In figure 1(a), with the increase of B_4C, the intensity of the main diffraction peaks of SiC (2θ=35.65°) and graphite (2θ=26.5°) decreases; and part of diffraction peaks of the SiC and Al_2O_3 disappears when the B_4C doping amount is 9%. When the heat treatment temperature increases to 1450 °C, as shown in figure 1(b), the SiC diffraction peak intensity increases with the rising of B_4C, indicating that the crystallinity of SiC in the refractory material grows and the amount of generation increases. The results suggest that B_4C at the heat

treatment temperature of 1450 °C contributes to improve the crystallinity of generated SiC as well as graphitization.

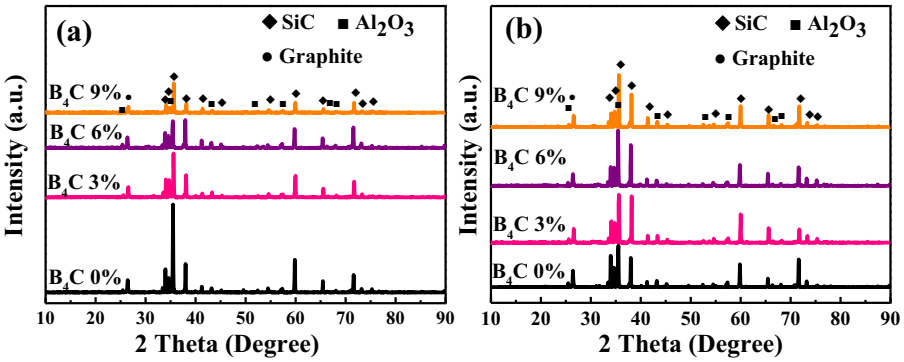

Figure 1. XRD patterns of SiC refractory ceramics with different B_4C content.

The graphitization degree of SiC-based refractory ceramics at different B_4C additions is characterized by Raman spectroscopy. Figures 2(a, b) show the Raman patterns of SiC-based refractory ceramics at 0% and 6% B_4C additions after heat treatment at 1450 °C. As can be seen from the figures, four distinct broad peaks can be observed, where the peaks at 1350 cm^{-1} and 1580 cm^{-1} can in turn be fitted to four folded peaks. The D peak represents lattice defects of carbon atoms in graphite, the G peak represents in-plane stretching vibrations of carbon atom sp2 hybridization. I_D/I_G is an vital indicator of graphitization degree [14], and the I_D/I_G of SiC refractory ceramics with different B_4C additions are calculated, where the I_D/I_G at 0% and 6% B_4C are 1.08 and 0.87, respectively, with the inclusion of B_4C, the graphitization degree increases significantly.

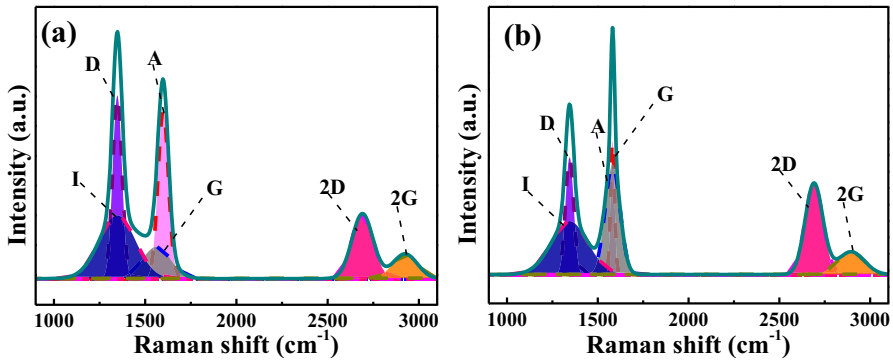

Figure 2. Raman patterns of SiC refractory ceramics with different B_4C content.

The SEM spectra of the SiC-based refractory ceramics with different B_4C content is shown in figure 3. In figure 3(a), the SiC-based refractory ceramics without B_4C shows a large number of apparent porosity in the fracture after heat treatment at 1100 °C. When the heat treatment temperature increases to 1450 °C, as shown in figure 3(b), the sample shows a significant increment in apparent porosity along with a small amount of needle-like structures. Figure 3(c) shows that when the B_4C content is 6%, there is apparent

sintering leading to densities; also, the EDS energy spectrum indicates the presence of B elements at the sintered dense. After heat treatment at 1450 °C, the inter-particle sintering is tight, while a small amount of SiC whiskers appeares as seen in figure 3(d), indicating that B_4C not only promotes the sintering of SiC-based refractory ceramics, but also the growth of SiC whiskers.

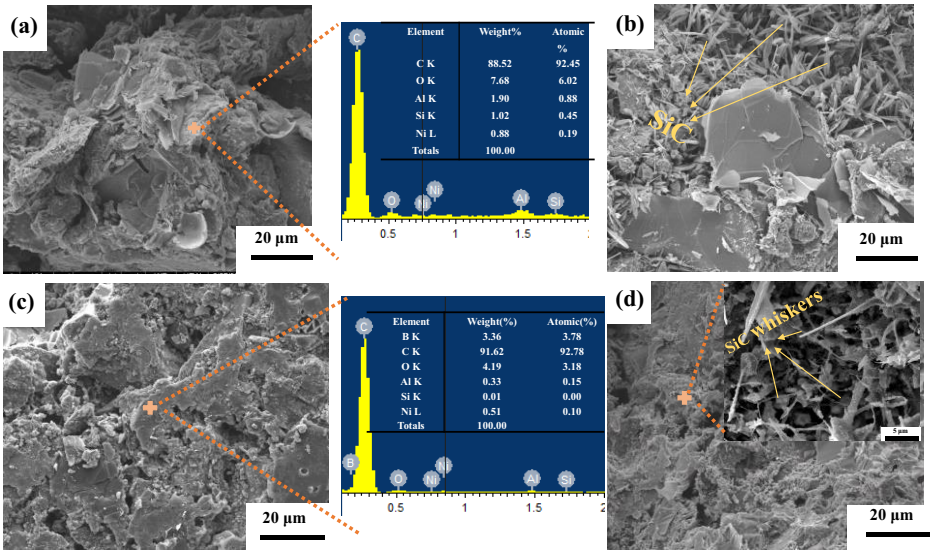

Figure 3. SEM patterns of SiC refractory ceramics with different B_4C content.

3.2. Characterization of the Properties of SiC-based Refractory Ceramics

Figure 4 illustrates the apparent porosity, bulk density, and linear change of SiC-based refractory ceramics after heat treatment at 1100 °C and 1450 °C for different B_4C content. From figures 4(a, b), it can be seen that the apparent porosity of the refractory decreases and the bulk density increases with the introduction of B_4C, which is consistent with the microstructure mentioned above. When the content of B_4C is 6%, the apparent porosity decreases from 17.1% to 10.97% after heat treatment at 1100 °C; and the corresponding bulk density increase from 2.50 g/cm^3 to 2.57 g/cm^3. The apparent porosity decrease from 16.63% to 15.2% after heat treatment at 1450 °C, and the bulk density increase from 2.51 g/cm^3 to 2.54 g/cm^3 after heat treatment at 1450 °C.

Figure 5 shows the cold modulus of rupture, cold compressive strength and oxidation index of SiC-based refractory ceramics after heat treatment at 1100 °C and 1450 °C for different content of B_4C. The change trends of cold modulus of rupture and cold compressive strength is approach. As shown in figure 4(a), when the B_4C addition raises from 0% to 6%, the cold modulus of rupture of SiC-based refractory ceramics increases from 18.88 MPa to 39.67 MPa and from 28.06 MPa to 50.25 MPa by 1100 °C and 1450 °C, respectively.

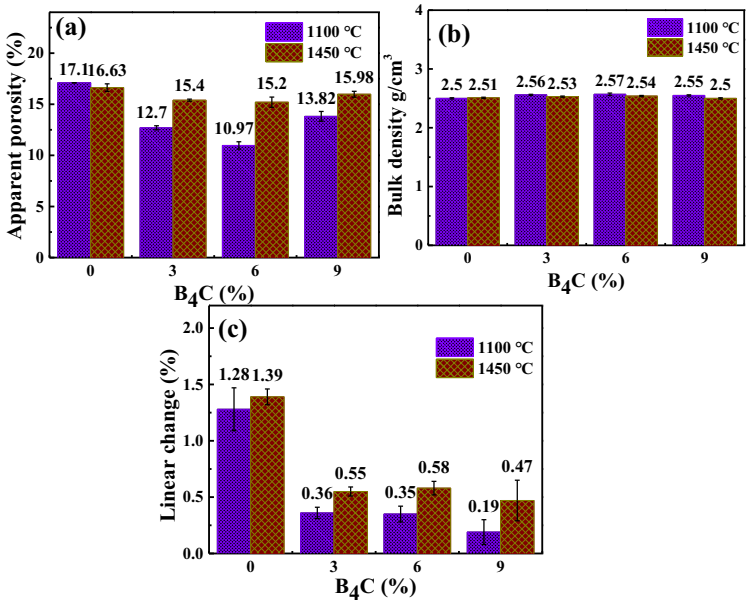

Figure 4. Apparent porosity, bulk density and linear change of SiC refractory ceramics with different B_4C content.

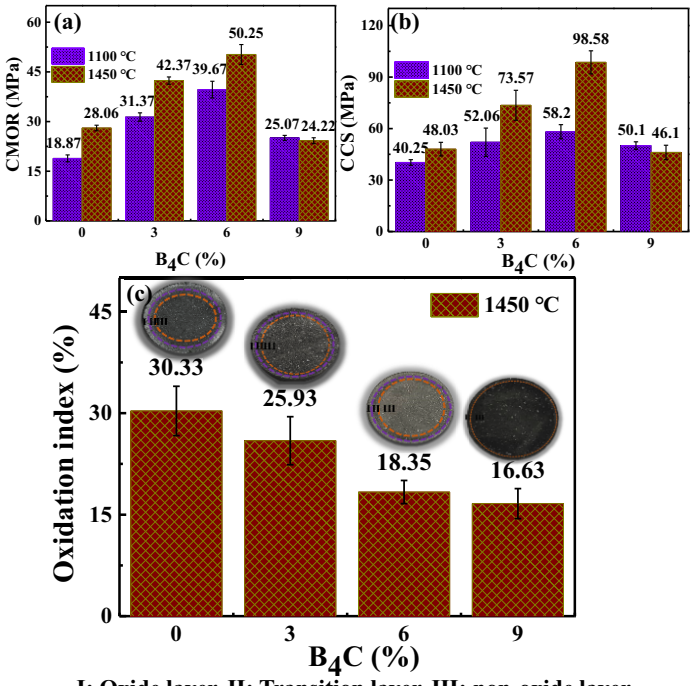

Figure 5. Cold modulus of rupture (CMOR), cold compressive strength(CCS) and oxidation index of SiC refractory ceramics with different B_4C content.

The cold compressive strength of SiC-based refractory ceramics increased from 40.25 MPa to 58.20 MPa and from 48.03 MPa to 98.58 MPa by 1100 °C and 1450 °C from figure 5(b), respectively. In figure 5(c), the oxidation index of the refractory without B_4C is 30.33%, and the presence of a large amount of white oxide at the refractory interface can be seen in the macroscopic photograph. When the B_4C addition is 9%, the oxidation index of the refractory is 16.63%, and the macroscopic cross-section is basically black without an obvious oxidation layer.

4. Conclusion

The conclusions of this paper are as follows: the introduction of B_4C can fill the pores between the particles and improve the crystallinity of SiC and graphitization. The apparent porosity of the refractory decreased from 16.63% to 15.20%, the bulk density increased from 2.51 g/cm^3 to 2.54 g/cm^3, and the linear change decreased from 1.39% to 0.47% after heat treatment at 1450 °C. The cold modulus of rupture and cold compressive strength of the refractory at a heat treatment temperature of 1450 °C with 6% B_4C content are 50.25 MPa and 98.58 MPa, respectively; the oxidation index is reduced from 30.33% to 16.63%.

Acknowledgments

This work is supported by the Science Fund for Creative Research Groups of the National Natural Science Foundation of Hubei Province (Grant No.2020CFA038), and the Key Research and Development Project of Hubei Province (Grant No. 2020BAA028).

References

[1] Cheng S, Yang T, Xue Q, Zuo H, Gao X, Yang W. Optimum design and layout of the cooling apparatus for long compaignship blast furnace. Int. J. Miner. Metall. Mater. 2003 Aug; 10(4): 24-28.
[2] Yeh CP, Ho CK, Yang RJ. Conjugate heat transfer analysis of copper staves and sensor bars in a blast furnace for various refractory lining thickness. Int. Commun. Heat Mass Transf. 2012 Jan; 39(1): 58-65.
[3] Wu R, Zhou K, Yue CY, Wei J, Pan Y. Recent progress in synthesis, properties and potential applications of SiC nanomaterials. Prog. Mater. Sci. 2015 Jul; 72: 1-60.
[4] Chen A, Fu Y, Mu Y, Wang Q, Parr C, Ye G. Oxidation resistance of andalusite-bearing Al_2O_3–SiC–C castables containing reduced anti-oxidant. Ceram. Int. 2021 May; 47(10): 14579-14586.
[5] Ding D, Tian X, Ye G, Touzo B, Ahouanto F, Parr C. Effect of andalusite aggregates on oxidation resistance of Al_2O_3–SiC–C castables. Ceram. Int. 2019 Oct; 45(15): 19237-19241.
[6] Li M, Tong S, Luo H, Li S, Chen R, Li C. Dual-functional application of Al_2O_3–B_2O_3 composite bubble in Al_2O_3–SiC–C castables as antioxidant and mechanical reinforcement agents. Ceram. Int. 2021 Aug; 47(16): 23686-23690.
[7] Cai Y, Fan S, Yin X, Zhang L, Cheng L, Wang Y. Microstructures and mechanical properties of three-dimensional ceramic filler modified carbon/carbon composites. Ceram. Int. 2014 Jan; 40(1): 399-408.
[8] Cai Y, Yin X, Fan S, Zhang L, Cheng L, Wang Y, Yin H. Effects of particle sizes and contents of ceramic fillers on tribological behavior of 3D C/C composites. Ceram. Int. 2014 Nov; 40(9): 14029-14037.
[9] Gogotai YG, Yaroshenko VP, Porz F. Oxidation resistance of boron carbide-based ceramics. J. Mater. Sci. Lett. 1992 Jan; 11(5): 308-310.
[10] Campos KS, e Silva GFL, Nunes EH, Vasconcelos WL. The influence of B_4C and MgB_2 additions on the behavior of MgO-C bricks. Ceram. Int. 2012 Sep, 38(7): 5661-5667.
[11] Magnani G, Beltrami G, Minoccari GL, Pilotti L, Pressureless sintering and properties of a SiC-B_4C composite. J. Eur. Ceram. Soc. 2001 May; 21(5): 633-638.

[12] Ma HB, Liu HL, Zhao J, Xu FF, Zhang GJ. Pressureless sintering, mechanical properties and oxidation behavior of ZrB2 ceramics doped with B_4C. J. Eur. Ceram. Soc. 2015 Sep; 35(10): 2699-2705.
[13] Fan S, He L, Yang C, Li H, Wang S, Lin Y, Cheng L. Effect of B_4C on the microstructure and properties of B4C modified three-dimensional needled C/C-SiC composites. Mater. Sci. Eng. A. 2017 Oct; 706: 201-210.
[14] Chen F, Luo H, Cheng Y, Guo R, Yang W, Wang X, Gong R. Nickel/Nickel phosphide composite embedded in N-doped carbon with tunable electromagnetic properties toward high-efficiency microwave absorption. Compos. Part A Appl. Sci. Manuf. 2021 Jan; 140: 106141.